

1 Using ^{10}Be to determine long-term erosion rates in Panama

2

3 Veronica Sosa-Gonzalez¹, Paul R. Bierman^{1,2}, Kyle K. Nichols³, Dylan H. Rood⁴

4

5 ¹Rubenstein School of the Environment and Natural Resources, University of Vermont ²Department of
6 Geology, University of Vermont ³Department of Geosciences, Skidmore College ⁴Lawrence Livermore
7 National Laboratory

8 **Abstract**

9 Using measurements of in situ produced ^{10}Be in river sediment we calculated erosion rates for
10 40 watersheds in Panama. A total of 44 variables (physiographic, climatic, seismic, geology and
11 a land use proxy) were quantified for each watershed and their relationship to erosion rates was
12 assessed using simple linear regressions and Analysis of Variance. Grain size analysis was used
13 to assess the impact of landslides on the concentration of ^{10}Be in fluvial sediment and thus on
14 erosion rates.

15 Cosmogenic ^{10}Be -inferred erosion rates ranged from 26 to 600 m/Myr . The strongest and most
16 significant relationship in the dataset was found between erosion rate and silicate weathering
17 rate, the mass of material leaving the basin in solution ($R^2=0.726$, $p = 0.004$, $n=9$). None of the
18 physiographic variables showed a significant relationship with erosion at the 95% significance
19 level. Three seismic variables were weakly and negatively related to erosion rates: average
20 magnitude of seismic events in a 75-km buffer ($R^2=0.550$, $p < 0.005$), average depth of seismic
21 events in a 50-km buffer ($R^2=0.466$, $p = 0.002$) and average magnitude of seismic events in a
22 25-km buffer ($R^2=0.431$, $p = 0.005$). An inverse relationship was found between ^{10}Be
23 concentration and grain size in landslide-related samples. Deep-seated material carries less ^{10}Be
24 than surface material.

25 Erosion rates in Panama are higher than all other published cosmogenic-derived erosion rates in
26 tropical climates including those from Puerto Rico, Madagascar and Sri Lanka. Many studies
27 have concluded that physiographic controls are related to erosion. The lack of such relationship
28 in Panama suggests a complexity in erosive dynamics.

29 Keywords: long-term erosion rates, Panama, physiography, seismic controls, landslide input

30

31 **1. Introduction**

32 Quantification of erosion rates, and knowledge of the factors that determine and impact
33 them, are important to many disciplines including aquatic ecology, geomorphology, economics,
34 and natural resources management. For example, sedimentation of waterways, an effect of
35 accelerated erosion, is associated with deterioration of water quality including increased turbidity
36 and temperature, and changes in dissolved oxygen concentration (Bilotta and Brazier, 2008). The
37 yield of water reservoirs can be affected by erosion because their capacity decreases as they fill
38 with sediment (Harden, 2006).

39 The effects of physiographic controls on erosion and sediment movement have been long
40 debated. Watershed elevation appears to exert control on erosion at a global (Portenga and
41 Bierman, 2011) and at a site-specific scale (Palumbo et al., 2009). Portenga and Bierman (2011)
42 found that mean basin slope significantly and positively relates to drainage basin erosion rates at
43 both local and global scales, and that relief is important in controlling erosion rates in the tropical
44 climate zones. However, von Blanckenburg (2004) concluded that relief alone does not lead to
45 accelerated erosion.

46 Cosmogenic isotopes, such as ^{10}Be , are formed when the earth materials are exposed to
47 cosmic rays (Lal and Peters, 1967). These nuclides provide a robust method to quantify erosion
48 rates, because they integrate enough time to average out extreme events on decadal and
49 centennial time scale, integrating erosion rates over 10^3 to 10^5 years. Production of *in situ*
50 cosmogenic isotopes decreases exponentially with depth and is in general inconsequential below
51 2 meters depth in rocks (Lal and Peters, 1967). Because of this, ^{10}Be is a good indicator of the
52 near-surface residence time of materials and hence, the rate at which Earth's surface is eroding.
53 Such long-term data can help place human influences on the landscape and its processes in
54 context (Bierman and Nichols, 2004; von Blanckenburg, 2005). This research will investigate
55 the importance of sediment delivery to rivers by discrete landslide events by doing grain-size
56 specific ^{10}Be analysis. Fine material located at the surface has been exposed to cosmic radiation
57 longer than coarser material at depth. Coarser material from landslides is expected to have lower
58 isotopic concentrations.

59 Our research aims to determine long-term, background erosion rates in Panama using
60 ^{10}Be measured in quartz extracted from river sediments (Figure 1). More than 88 studies using
61 ^{10}Be as a proxy for erosion rate; however, just a few studies have been done in tropical
62 environments. Portenga and Bierman (2011) compiled all published data on cosmogenic-derived
63 erosion rates and only 98 of 1599 are from tropical river sediment samples. Of all tropical
64 samples, 17 were obtained in Panama. This research expands the breadth of environments where
65 cosmogenic isotopes have been measured and provides important information for the
66 management of the Panama Canal, in particular, the lifetime of the reservoirs integral to canal
67 operation. Our study presents erosion rate data for 40 Panamanian watersheds and thus the first
68 country-scale determination of background erosion rates in Panama.

69 Using the ^{10}Be -estimated erosion rates, we place human impact in the context of
70 background erosion rates and gain knowledge about the relationship of erosion rates, in a tropical
71 climate, to physiography, tectonic activity, geology and biologic features. Assessing these
72 relationships demonstrates the lack of physiographic controls on erosion rates in tropical
73 climates.

74 **1.1 Regional Setting**

75 1.1.1 Study area

76 Panama is the southernmost Central American country. The country comprises an area of
77 75,517 km² (Contraloría General de la República de Panamá, 2008). It is bounded on the north
78 by the Caribbean Sea, on the south by the Pacific Ocean; on the east it shares borders with
79 Colombia and on the west with Costa Rica (CGRP, 2008).

80 1.1.2 Geography and Climate

81 Panama has low-relief coastal plains and a more rugged Central Cordillera extending
82 along most of the isthmus from the border with Costa Rica to the Panama Canal (Palka, 2005).
83 Maximum elevations are located in the southwestern province of Chiriquí: Barú volcano
84 (3,475m) and Cerro Picacho (2,986m) and the northwestern province of Bocas del Toro: Cerro
85 Fábrega (3,335m), Cerro Itamut (3,279m) and Cerro Echandi (3,162m) (CGRP, 2005). Rivers
86 draining into the Caribbean Sea average 56 km in length, and have an average slope of 5.5%.
87 Their discharge volume is greater than those draining to the Pacific, because of their short
88 distance from mountains to sea. Rivers draining to the Pacific Ocean average 106 km in length,
89 and have lower slopes, averaging 2.27% (CGRP-INEC, 2005).

90 Climate in Panama is tropical maritime with influences from the Caribbean Sea and Pacific
91 Ocean (Contraloría General de la República de Panamá- Instituto Nacional de Estadística y
92 Censo, 2005). The climate is characterized by high year-round temperatures, with low diurnal
93 and annual range, abundant precipitation, and high relative humidity. Temperatures are high
94 year-round. Annual mean temperatures range between 24°C and 28°C. The average diurnal
95 temperature range is approximately 1.9°C on the Caribbean slopes and ranges between 1.5 and
96 2.9°C on the Pacific side (CGRP-INEC, 2005).

97 Generally, there are two seasons: wet and dry; the wet season goes from May to
98 December, and the dry one from December to April (CGRP-INEC, 2005). The Pacific's side
99 mean annual precipitation ranges from 1,500 to 3,500mm, and there is a marked difference
100 between the dry and wet seasons. On the Caribbean slope, precipitation is more uniform year
101 round, exceeding 4,000mm annually and with no marked difference between the seasons.

102 1.1.3 Tectonic setting and geology

103 Panama is geologically young. The isthmus where Panama is located resulted from
104 collision of the Panama-Choco island arc with South America. This took place in the late
105 Miocene-Pliocene (3.5-7 million years ago). Adamek and others (1988) suggested the existence
106 of a microplate (the Panama-Costa Rica microplate) that includes most of Costa Rica. It shares
107 borders with the Caribbean plate on the north, the Cocos plate on the southwest, the Nazca plate
108 to the south, and the South American plate to the east and southeast (Camacho et al., 1997).

109 Camacho et al. (1997) conducted a seismic hazard assessment for Panama, and produced
110 peak ground acceleration maps. The highest seismic hazard and ground acceleration is on the
111 western side of the country, close to the Panama Fracture Zone and the western segment of the

112 North Panama Deformed Belt; and to the southeast of the country close to the Panama Block-
113 South America plate margin. The lowest seismic hazard is in Central Panama. The Pacific side is
114 characterized by its geologic activity, having a deep oceanic trench, narrow marine shelf and
115 active subduction (responsible for volcanic activity and earthquakes). The Atlantic side is a
116 passive, stable margin with a broad marine shelf (Harmon, 2005).

117 Panama is mostly composed of volcanic rocks. The Canal Zone is mostly underlain by
118 volcanic tuffs from the Miocene era. These can also be found in the eastern region of Darien.
119 The geology of eastern Panama consists mostly of volcanic tuffs and ashes, with small areas of
120 limestone. There are regions on the east where limestone is interbedded with dark clay shale
121 formations and sandstone. A region of tuffs, ash and lava blended with marine and terrestrial
122 sediments extends west from the central Canal Zone. To the west, by the province of Bocas del
123 Toro, the sedimentary column includes limestone-volcanic series of Eocene age as well as
124 conglomerates, sandstones, shales and sandy limestones of Miocene age (Schuchert, 1935; Terry,
125 1956).

126 Metamorphic rocks are scarce. Schist has been reported on the eastern province of
127 Darien. Small slate outcrops have been reported in several provinces stretching from the center
128 to the west, close to the Costa Rica border. Sedimentary rocks are mostly limited to the eastern
129 region of Panama with a few exceptions on the west.

130 **2. Methods**

131 2.1 Basin selection and sampling

132 Samples used in this study were collected by Russell S. Harmon and Kyle K. Nichols in
133 three field seasons: 2004, 2007 and 2009. A total of 55 samples river samples were collected, of
134 which 16 could not be analyzed for ^{10}Be , due to their low quartz content.

135 The 2004 samples were collected in the upper Chagres River, the sediment yield of which
136 was measured between 1981 and 1996 to test for human impact, specifically, deforestation. The
137 Chagres River is essential to the Panama Canal as it fills one of the main reservoirs integral to
138 canal function. Samples on the northern side of the divide, draining to the Caribbean Sea, were
139 collected to test whether average basin slope controlled erosion rates. Three rivers in this region
140 were sampled multiple times along their length. These were Rio Nombre de Dios, Cuango and
141 Pequini. In 2007, samples were collected by Nichols along the Pan-American Highway north of
142 Panama City, where the road was crossed by rivers. Russell Harmon and Steven Goldsmith were
143 conducting research on the chemical weathering in Panama (Harmon, personal communication),
144 and collected sediment samples that were used in our research.

145

146 Four samples were collected in 2009, three related to a landslide. One was a temporal
147 replicate for the Rio Chagres, previously sampled in 2002. One sample was collected from
148 landslide material, one sample upstream from the confluence of the river and the landslide, and
149 one from the river channel downstream of the landslide. These last three samples were then
150 divided into 7 grain size splits each, making a total of 21 landslide-related samples.

151 2.2 Laboratory methods

152 Samples were dried and sieved. Coarse grain-size splits were pulverized using a plate
153 grinder. The 3 landslide-related samples were all analyzed for ^{10}Be content by size fraction:

154 <0.25mm, 0.25-1mm, 1-2mm, 2-4mm, 4-9mm, 9-12mm, and >12mm. River sediment samples
155 (unrelated to the landslide) were divided into 3 size fractions: <0.25mm, 0.25-0.85mm, and
156 >0.85mm. Only the 0.25-0.85mm split was chemically treated to isolate quartz and extract ^{10}Be .
157 Samples were chemically treated to isolate the quartz and remove meteoric ^{10}Be following the
158 method of Kohl and Nishiizumi (1992).

159 Samples of purified quartz were spiked with Be and Al carrier, to reach desirable total
160 element loads (2500 μg Al and 250 μg Be), and dissolved in hydrofluoric acid. Digestion of the
161 samples took place with increasing heat over the course of two days until the quartz dissolved
162 completely. Samples were treated with perchloric and hydrofluoric acid dry downs to prepare
163 them for anion chromatography, where they were stripped of iron. A solution of weak sulfuric
164 acid and hydrogen peroxide prepared the samples for cation chromatography which divided the
165 sample into aluminum and beryllium fractions. Titrations with ammonium hydroxide, using
166 methyl red as an indicator, neutralized the acid in the sample and precipitated the Be fractions
167 into hydroxide jells. Jells were dried, the BeOH oxidized over a flame to BeO , and the oxide
168 packed into metal targets after being mixed in a 1:1 molar ratio with niobium (Hunt et al., 2006).

169 2.3 ^{10}Be measurement and erosion rates calculations

170 Isotopic ratios were measured using Accelerator Mass Spectrometry (AMS) at Lawrence
171 Livermore National Laboratory (LLNL). Blank corrections were made based on fully processed
172 blanks. Erosion rates based on the isotopic data were obtained using the CRONUS Earth
173 Calculator Version 2.2 (<http://hess.ess.washington.edu/>). Watersheds were delineated in ArcGIS
174 9.2, based on a 30-DEM and their effective elevation was obtained (Portenga and Bierman,
175 2011).

176 Erosion rates obtained from CRONUS were highly skewed so they were logarithmically
177 transformed (\log_{10}) in order to be able to perform parametric statistical analysis (Figure 2).
178 Because no spatial pattern of erosion rates was evident across Panama, watersheds were grouped
179 according to their region. Five regions resulted from this clustering: southwestern region (3
180 watersheds), northwestern (5 watersheds), central (7 watersheds), central-eastern (8 watersheds),
181 and eastern (17 watersheds). For statistical analysis of the regions, physiographic and climatic
182 parameters for all the watersheds were averaged, except for the number of seismic events, for
183 which the sum of the events in all watersheds was used for parametric analysis.

184

185 2.4 Data Analysis

186 A Geographical Information System (GIS) was used to quantify landscape
187 (physiographic, climatic, seismic and land use) variables and study the spatial distribution of
188 erosion rates. All spatial information was projected in NAD 1927 Zone 17N (previously
189 denominated Canal Zone). Gaps in the 90-meter resolution SRTM Digital Elevation Model
190 (DEM) used for watershed delineation were corrected using the USGS GTOPO30. The corrected
191 DEM was used to quantify slope, area, and relief. A digitized map of Panama's geology was
192 obtained from Smithsonian Tropical Research Institute. Peak Ground Acceleration (PGA) for
193 each watershed was obtained based on data produced by the Global Seismic Hazard Assessment
194 Program and downloaded from their website (<http://www.seismo.ethz.ch>) The amount of seismic
195 events from 1900-2011, as well as average depth and magnitude of seismic events in each
196 watershed, were extracted from a seismic catalog from the Instituto de Geociencias de Panamá
197 (Dr. Eduardo Camacho, personal communication). Climatic data (19 variables) was developed

198 by WorldClim and obtained from their website (<http://www.worldclim.org>). Isothermality,
199 included in the climatic data, is a measure of the annual temperature range experienced on a
200 daily basis (Varela, 2009).

201 Data were entered into an SPSS database for simple linear regressions and analysis of
202 variance relating erosion rates to landscape metrics. IBM SPSS Statistics 20 was used for these
203 analyses.

204

205 **3. Results**

206 **3.1 River sediment samples**

207 The concentration of *in situ* ^{10}Be measured in Panamanian river sand varies widely from
208 7.4 ± 1.6 to $139 \pm 3 \times 10^3$ atoms/g (Table 1, 1 standard deviation (SD) here and elsewhere in the
209 paper). When samples were grouped by region, quartz extracted from rivers in the southwestern
210 region had the lowest ^{10}Be concentration ($8.37 \pm 1.27 \times 10^3$ atoms/g). The lowest concentration
211 of ^{10}Be measured as part of this study was in the river sediment of the Rio Bartolo (BART), in
212 the southwestern region (Table 2). Samples from the central-eastern region had an average ^{10}Be
213 concentration of $64.0 \pm 46.6 \times 10^3$ atoms/g. The variance in the central-eastern region was the
214 largest of all regions (72% SD). The mean ^{10}Be concentration was significantly different between
215 the eastern and central-eastern region ($p = 0.007$) but no significant differences were found in
216 mean ^{10}Be concentrations for stream sediment between other regions as shown by ANOVA.

217 Erosion rates, inferred from the concentration of *in situ* produced ^{10}Be , range from $26.1 \pm$
218 0.6 m/Myr to $597 \pm 62 \text{ m/Myr}$ (Table 1); the average rate for the 35 rivers we sampled is 218

219 m/Myr \pm 151 m/Myr, the area-weighted average is 150 m/Myr. The most slowly eroding basins
220 are generally found in the central-eastern region, and rapidly eroding basins are scattered through
221 the country (Figure 3). When samples were grouped by region, the southwestern region had the
222 highest average erosion rates; however, the central region has the biggest variance in erosion
223 rates because of the outlier (FELIX); if that extreme value is not taken into account, the eastern
224 region has the greatest variance (Figure 4). Average erosion rate for the southwestern region is
225 significantly different from the average erosion rate of the central ($p = 0.020$) and central-eastern
226 regions ($p = 0.003$). All other differences were not significant.

227 Two rivers, the Pequini and Chagres were sampled multiple times along their length to
228 assess spatial variations in erosion (Figure 5). A sample from the Pequini headwaters (PHW) was
229 7.40km away from the sample extracted before the confluence of the Pequini with the Rio San
230 Miguel (PSM), and 13.3km away from a sample taken at the outlet of the watershed (PLA).
231 Erosion rates calculated for the three nested watersheds showed a 13 percent standard deviation.
232 The upper Rio Chagres was sampled in 2009 (CHAG2009), and a landslide on the Chagres
233 watershed. Amalgamated samples from upstream of the landslide were combined to represent a
234 sediment sample (PLS) that included the watershed for CHAG2009. Erosion rates calculated for
235 both segments of the upper Rio Chagres (PLS and CHAG2009) differed by a percent standard
236 deviation of 71 (Table 3).

237 Two rivers were sampled in similar locations but at different times. The Rio Nombre de
238 Dios was sampled in 2004 (NDD) and 2007 (DIOS), and so was the Rio Cuango (CUAN, 2004;
239 CNGO, 2007). A smaller variation between samples was found in the Rio Nombre de Dios,
240 (6%) than the Rio Cuango, 23%. Erosion rates were calculated for the area between

241 subcatchments (Table 4). In general, inferred ^{10}Be content and erosion rates of the
242 subwatersheds were similar.

243 In general, bivariate linear regression analysis showed few statistically significant
244 relationships between watershed scale erosion rates inferred from ^{10}Be measurements and
245 landscape scale variables (i.e., physiographic, climatic, geology, seismic and land use; Table 5).
246 There were no significant relationships between erosion rates and physiographic metrics (area,
247 slope, and relief). Several bioclimatic variables showed weak but positive relationships with
248 erosion rates including temperature seasonality ($R^2= 0.445$, $p= 0.004$), and precipitation during
249 both the driest month ($R^2= 0.319$, $p= 0.045$) and the driest quarter ($R^2= 0.376$, $p= 0.017$). Two
250 bioclimatic variables showed a weak negative relation to erosion rates: isothermality ($R^2= 0.381$,
251 $p= 0.015$) and precipitation seasonality ($R^2= 0.394$, $p= 0.012$). Tree cover was used a land use
252 proxy, and it showed a negative relation with erosion rates ($R^2= 0.351$, $p= 0.026$).

253 The relationship between erosion and seismicity was tested using six arbitrarily chosen
254 buffer distances (100m, 10km, 25km, 50km, 75km and 100km) to examine changes, if any, in
255 seismic control of erosion rates as a function of distance from the watershed. These buffers were
256 applied to each delineated watershed and seismic variables were quantified within each buffer.
257 The strongest relationships with seismicity are negative (Table 6). The average magnitude of
258 seismic events showed a relationship at a 75km buffer from the watersheds ($R^2= 0.550$, $p<0.005$)
259 and at the 25km buffer ($R^2= 0.431$, $p= 0.005$). Within a 50km buffer, the strongest relation was
260 found between erosion rates and the average depth of the events ($R^2= 0.466$, $p= 0.002$). Other
261 weak relationships were found with the 25km, 50km, 75km and 100km buffers. No significant
262 relationships were found at the 100m and only one at the 10km distance.

263 The strongest relationship was found between physical erosion rates and chemical
264 weathering of silicate rocks ($R^2 = 0.558$, $p = 0.021$, $n = 9$). In Panama, silicate weathering
265 accounts for roughly 2-18% of the total denudation (Table 7). Stepwise regression results in a
266 model that includes both chemical weathering and precipitation of the driest month as
267 explanatory variables ($R^2 = 0.915$, $p = 0.001$).

268 Although erosion rates and landscape scale parameters are not well correlated at the basin
269 scale, they are better correlated if considered at a regional scale. Clustering samples into regions
270 and assessing their relationship to parameters, shows an increase in correlation coefficients,
271 except for mean annual precipitation, which decreases. However, when only five samples
272 (geographical regions) are considered for analysis, the test has low power. As a result of this, p-
273 values increase and the relationships are no longer statistically significant.

274

275 3.2 Landslide samples

276 ^{10}Be concentration in the grain size fractions of all landslide-related sediment samples
277 ranged from 7.33 ± 0.40 to $39.1 \pm 1.71 \times 10^3$ atoms/g, on the low end of concentrations
278 measured as part of this study. Grain size and *in situ* ^{10}Be concentration are inversely related
279 (Figure 6). Individual linear regressions showed that they are well correlated ($R^2 = 0.600$; $p <$
280 0.005). The isotopic concentration of the landslide material is less than that for the upstream and
281 downstream material, in almost all size fractions, except for >12mm.

282 Sediment upstream of the landslide contains more ^{10}Be than sediment downstream.
283 Analysis of variance showed that the relationship between ^{10}Be content and grain size is
284 statistically significant ($F = 4.175$; $p = 0.013$). Based on visual examination of the trend observed

285 in the graph of ^{10}Be concentration as a function of grain size, size fractions were grouped into 4
286 categories to test for differences in isotopic concentrations: <0.25mm-1mm, 1-2mm, 2-9mm, and
287 >9mm. Using these categories, an ANOVA was run, and a stronger relationship between isotopic
288 concentration and grain size was found ($F=9.536$, $p = 0.001$). Mean isotopic concentration of the
289 <0.25mm fraction is statistically different from all the fractions greater than 2.00mm at the 0.05
290 level. No relationship holds between ^{10}Be concentration and sediment source ($F= 2.193$; $p =$
291 0.141), but there is an evident difference in their average ^{10}Be concentration. Using a two-
292 component mixing model suggests that the landslide accounts for 50% of the sediment just
293 downstream of the slide.

294 **4. Discussion**

295 Basin-scale erosion rates in Panama vary over more than an order of magnitude and are
296 in general, quite rapid, averaging several hundred meters per million years. Erosion rates are
297 largely unrelated to topographic metrics, vary in a coherent spatial pattern, and are correlated to
298 various expressions of tectonic activity. Physical erosion rates and chemical weathering of
299 silicate rocks are well correlated.

300 4.1 Comparison to other cosmogenic studies

301 Erosion rates of Panamanian basins span much of the range previously reported for
302 tropical basins. Forty watersheds in Panama, some of which are nested and vary in area from
303 13.6 km^2 to $2,410 \text{ km}^2$, had erosion rates that range from $26.1 \pm 0.6 \text{ m/Myr}$ to $597 \pm 62 \text{ m/Myr}$.
304 The average erosion rate for the Panamanian watersheds considered in this study is significantly
305 higher than that for other tropical regions including Puerto Rico, Madagascar, and Sri Lanka
306 ($F=19.767$, $p < 0.005$; Figure 7) (Brown et al., 1995; Brown et al., 1998; Cox et al., 2009,

307 Hewawasam et al., 2003; von Blanckenburg et al., 2004). Watersheds included in those tropical
308 studies, ranged in area from 0.02 to 134.6 km² with most less than 50 km². Panama's dataset is
309 extensive when compared to other tropical studies; the number of samples included in those
310 studies ranges from 4 to 10, whereas the Panama dataset has 40 watershed samples.

311 Erosion rates have been determined in Puerto Rican watershed, in two separate studies.
312 Brown et al. (1995) determined an average erosion rate of 61.7 ± 41.3 m/Myr for the Rio Icacos.
313 In 1998, Brown et al. determined the erosion rates for the Quebrada Guabá (50.8 ± 27.7 m/Myr)
314 and Rio Cayaguás (70.1 ± 19.9 m/Myr). Average erosion rates in tropical Madagascar (n = 4) are
315 13.9 ± 5.7 m/Myr (Cox et al., 2009). Two separate studies have quantified cosmogenically-
316 derived erosion rates in Sri Lanka. In 2003, Hewawasam et al. found that the average erosion
317 rate of six tropical subwatersheds of the Upper Mahaweli catchment was 21.1 ± 4.2 m/Myr. Von
318 Blanckenburg et al. (2004) reported an average erosion rate of 16.2 ± 7.0 m/Myr on the same
319 region in Sri Lanka (n=16).

320

321 When compared to these study sites, Panama is eroding faster than all of them. Seismicity
322 and tectonic setting differ between Panama, Madagascar, and Sri Lanka; the latter two are
323 located in a region with little tectonic activity. In contrast, Panama is located in an active tectonic
324 zone. Peak ground acceleration, defined as the magnitude of ground motion with a 10% chance
325 of being exceeded within 50 years, and expressed as a fraction of the acceleration due to gravity
326 (g) is 0.06 g for the 16 studied watersheds Sri Lanka, and 0.36 for Madagascar (Portenga and
327 Bierman, 2011). For Panama, mean peak ground acceleration in the 40 studied watersheds, is

328 more than an order of magnitude higher, ranging between 1.77 and 4.37 g (average: 2.29). In
329 Puerto Rico, peak ground acceleration averaged 1.88.

330

331 Using the data published by Portenga and Bierman (2011) and the data from this study, mean
332 temperature and precipitation were compared for tropical cosmogenic studies. Mean temperature
333 in the sampled Panamanian watersheds averaged 24.4 °C; in Sri Lanka, it averaged 19.2°C, in
334 Madagascar, 20.2°C and 21.6°C in Puerto Rico. Mean annual precipitation for the watersheds is
335 relatively similar in Panama, Puerto Rico and Sri Lanka, averaging 2796 mm, 2599 mm and
336 2480 mm respectively. They differ from Madagascar, where precipitation averages only
337 1134mm. Higher erosion rates are associated with elevated annual precipitation.

338

339 4.2 Relation to silicate weathering

340

341 The strongest and most significant relationship in our dataset was found between erosion
342 rates and chemical weathering of silicate rocks ($R^2= 0.726$, $p= 0.004$, $n= 9$). A positive
343 relationship between chemical and physical erosion has been found before by Riebe et al. (2003;
344 2004) and von Blanckenburg (2005).

345 In their study of the controls on chemical weathering in a variety of climate regimes,
346 Riebe et al. (2004) argued that there is a potential positive feedback between physical and
347 chemical erosion. Physical erosion depends, in part, on the chemical breakdown and weakening
348 of rocks as minerals alter, and chemical weathering depends on the availability of fresh mineral

349 surfaces created by physical erosion. In a study of physical erosion and chemical weathering in
350 Rio Icacos (Puerto Rico), Riebe et al. (2003) concluded that there is a tightly coupled
351 relationship between physical erosion and chemical weathering. Von Blanckenburg (2005) also
352 found that physical erosion and chemical denudation are related. That study compiled previously
353 published isotopic data and related it to physiographic metrics and chemical weathering data. He
354 found that the slope of the best fit line on the plot of chemical versus physical erosion rates was
355 0.2, supporting that there is a relationship between physical erosion and chemical weathering.
356 For Panama, we compared chemical and physical denudation and we find that the relationship is
357 strong ($R^2 = 0.726$, $p = 0.004$). Our data agrees with von Blanckenburg's findings, in that the
358 relationship between physical and chemical weathering is strong.

359

360 Von Blanckenburg et al. (2004) observed that while erosion rates in Sri Lanka are low, so
361 are silicate weathering rates. They attributed the low rate of silicate weathering to slow rates of
362 physical erosion, thereby limiting the supply of readily weathered material. However, they
363 concluded that silicate weathering represents a significant fraction of the total denudation. They
364 found that denudation rates ranged between 5 and 30 $t \text{ km}^{-2} \text{ yr}^{-1}$, and silicate weathering ranged
365 between 5 and 20 $t \text{ km}^{-2} \text{ yr}^{-1}$. In Panama, silicate weathering accounts for roughly 2-18% of the
366 total denudation. The remaining percentage can be attributed to material being washed out of the
367 basin.

368 West (2005) compiled previously published data on chemical weathering and physical
369 denudation for study sites across the world. Chemical weathering rates had been determined via
370 surface water chemistry and physical erosion using sediment fluxes or cosmogenic nuclides.

371 After comparing both datasets, he found that in a transport-limited environment (that is, when the
372 physical erosion is slow and limits the movement of chemically weathered material) total
373 denudation rate – chemical and physical- explains 94% of the variability in silicate denudation
374 rate.

375

376 A transport-limited environment is not likely to be found in Panama, where the physical
377 erosion rates are among the highest cosmogenic-derived ones ever published (Portenga and
378 Bierman, 2011). Because of this, silicate weathering is not expected to account for much of the
379 variability in the physical erosion rates.

380 4.3 Spatial scale of analysis

381 Both alone and together, none of the 45 landscape-scale metrics explained well the spatial
382 variation in Panamanian basin-scale erosion rates. Although some relationships were statistically
383 significant, there was large scatter (low R^2). When data were lumped at a regional scale, the
384 strength of the relationships (R^2) increased, but the statistical significance decreased (small n). A
385 similar trend of weakening relationship as the analysis scale increased was found globally by
386 Portenga and Bierman (2011). As the scale of analysis increases, so does the number of factors
387 that influence a certain phenomenon; also, factors are likely to interact with each other. This can
388 reduce the explanatory power of a single variable.

389 Because the cosmogenic nuclide method measures the concentration of ^{10}Be , one can test
390 effective sediment mixing within the watershed. A t-test comparing watersheds smaller than
391 100km^2 with those greater than 100km^2 in our dataset showed that there is no significant
392 difference in their average erosion rate ($t=-1.308$; $p = 0.306$). This lack of difference confirms

393 that sediment mixing is effective and that the erosion rate of small watersheds is on average no
394 different than that of large watersheds. Portenga and Bierman (2011) also found no relationship
395 between erosion rates and basin area with a much larger dataset.

396

397 4.4 Tectonics and seismicity

398

399 Of the seismicity proxies analyzed, several showed a significant relationship to erosion rates.
400 Average magnitude of the seismic events is inversely related to erosion at a variety of buffer
401 distances, suggesting that it is the most important seismic variable of the ones we analyzed.
402 Quantity of seismic events at the 10-km buffer was positively related to erosion rates. When
403 analyzing at the regional scale, the only significant relationship (of all metrics) is between the
404 number of seismic events in the 10-km buffer and erosion ($R^2 = 0.813$, $p = 0.036$). This
405 relationship is positive.

406

407 At the medium (25km) and large (75km and 100km) scale, the energy released during seismic
408 events is the important factor, at the medium scale (50km), it is the depth of the events and at a
409 shorter scale (10km), it is the number of seismic events, regardless of magnitude or depth. In the
410 immediate scale (100m buffer) none of the seismic variables is significantly related to erosion
411 rates. Western Panama has the greatest density (Figure 8). However, the events of greatest
412 magnitude occur outside of this region. This may explain the negative relation of erosion with

413 average magnitude of seismic events. Peak Ground Acceleration, another seismicity proxy,
414 showed a weak positive relationship with erosion rates ($R^2 = 0.096$, $p = 0.054$).

415 The density of seismic events is highest where some of the most rapidly eroding watersheds are
416 located (southwestern region). For example, the watershed for the Rio Felix (FELIX), which has
417 the highest erosion rate (598 m/Myr), located east of the region with a high frequency of seismic
418 events.

419

420 There is a spatial gap (where no erosion rates were determined) between the southwestern region
421 and the central region. A total of 10 samples were taken from this area, but due to their low
422 quartz content, no ^{10}Be analysis was done. Covering this spatial gap would be helpful in
423 identifying trends in erosion rates in that region. Because of this, it is difficult to reach any
424 specific conclusions from our data regarding the high erosion rate of Rio Felix and its
425 relationship to seismic activity.

426 One of the mechanisms by which erosion may be triggered due to seismicity is by increasing
427 landslide events. Recently, Ouimet (2008) studied the effect of M 7.9 earthquake on erosion in
428 China. As a result of the ground shaking associated with the earthquake, slope stability was
429 decreased. He concluded that the frequency of landslides increased erosion rates after the
430 earthquake.

431

432 In a study examining weathering and denudation in Sri Lanka, von Blanckenburg et al. (2004)
433 concluded that weathering and erosion were sensitive to base-level change resulting from
434 tectonic forcing but were not accelerated by increased precipitation and temperature.

435

436 Kong et al. (2007) observed the effect of climate and tectonics on long-term erosion rates in
437 Tibet. They compared the erosion rates for the Tibet to those in different climate regimes and
438 found them to be similar, suggesting that there is no climatic control on erosion. Their work
439 found a positive relationship between erosion and tectonics. They concluded that rock uplift, as a
440 result of tectonic activity in the Tibet region, is related to erosion. In a study of the coupling of
441 tectonics and erosion in the Western Alps, Malusá and Vezzoli (2006) concluded that regardless
442 of the lithology of the source area, most of the sediments produced in the region are due to
443 tectonically-related uplift.

444

445 Erosion may also be related to tectonic uplift in Panama. Davidson (2010) measured uplift rates
446 in the Burica Peninsula, on the border of Panama and Costa Rica, using GPS measurements. He
447 concluded that the Burica Peninsula is uplifting at a rate of ~55mm/yr. The southwestern region
448 we demarcated has the highest erosion rates in Panama and is located in the Burica Peninsula.
449 Although average erosion rates are 100 times less than uplift rates, rapid uplift in this area
450 suggests that increased denudation may be related to tectonic uplift.

451

452 It is important to point out that the response to seismic events may be tied to lithological
453 differences. This is hard to assess in Panama, where knowledge of the geology, hidden as it is
454 under deep jungle cover, is scarce, and the available digital information on surface geology and
455 bedrock is not detailed.

456

457 4.5 Topographic controls

458

459 Topographic variables (i.e., basin area, relief, slope, elevation) have been related to erosion rates
460 in many studies (see Summerfield and Hutton, 1994; Milliman and Syvitski, 1992). Erosion rates
461 of Panamanian watersheds does not appear to be related to elevation ($R^2 = 0.002$, $p = 0.804$),
462 relief ($R^2 = 0.038$, $p = 0.232$) or average basin slope ($R^2 = 0.000$, $p = 0.951$). Stepwise regressions
463 showed no relation between erosion rates and topographic variables. This means that no
464 combination of topographic variables or combination of a topographic and climatic (or other type
465 of) variable is significantly related to erosion.

466

467 These findings contrast with previously published work that concluded such relationships exist.
468 Summerfield and Hutton (1994) found a strong relationship between relief and mechanical
469 denudation rate. Local relief and runoff were the dominant controls on erosion in the large basins
470 they analyzed. Milliman and Syvitski (1992) concluded from their data that basin size and
471 topography are important controls of the export of sediment (sediment yield).

472 Riebe et al. (2001) used cosmogenic nuclides to measure erosion rates in seven topographically
473 different watersheds in Sierra Nevada, California. They argued that a lack of relationship
474 between topography and erosion rates may be indicative of equilibrium. If the base-level
475 lowering rates are uniform, hence the system is at equilibrium, hillslopes exerts no control on
476 erosion, and it is rather due to bedrock erodibility. On the other hand, when local base-level
477 lowering rates are variable (not in equilibrium), erosion rates are related to average basin slope.
478 This is a potential explanation for the lack of such relationships in Panama.

479 4.6 Climatic control

480 It has been thought that both the average precipitation and exceptional hydrologic events are
481 positively related to erosion rates (Milliman and Syvitski, 1992). However, for this research, 19
482 bioclimatic variables were considered, including maximum and minimum precipitation for each
483 watershed, and none had a statistically significant relation to erosion. Mean annual precipitation
484 exerts only a weak control in erosion at the basin scale. ($R^2 = 0.095$, $p = 0.057$). When regional
485 analysis was performed, this relationship got weaker. Temperature did not have significant
486 relationship with erosion either at the basin ($R^2 = 0.002$, $p = 0.807$) or the regional scale ($R^2 =$
487 0.016 , $p = 0.841$).

488

489 Riebe et al. (2001) concluded that climate exerted a minimal control on erosion in 7 watersheds
490 in Sierra Nevada, California. These watersheds varied in average temperature and precipitation
491 regime; none of these seemed to relate to erosion rates. From their research in Sri Lanka, von
492 Blanckenburg et al. (2004) suggested that increasing temperature alone does not accelerate
493 erosion rates. Findings of this research agree with the conclusions reached in both works.

494

495 4.7 Lithology

496

497 Analysis of Variance found no significant difference between the three geology classifications
498 considered (igneous intrusive, volcanic, and sedimentary rocks) and erosion rates at the 0.05
499 significance level ($F=2.469$; $p= 0.099$). The watersheds in the southwestern region, the fastest
500 eroding, coincide with sedimentary lithologies cropping out at the surface, similar to the finding
501 made in the world-wide dataset by Portenga and Bierman (2011). This is also the area where the
502 seismic activity is greater; this may imply a relationship between seismicity and the existence of
503 sedimentary basins. However, the relationship between sedimentary lithology and higher erosion
504 rates is significant only at the $p < 0.1$.

505 4.8 Grain size and isotopic concentration

506 My data suggest that sediment introduced to Panamanian rivers by landslides has lower ^{10}Be
507 concentrations than sediment entering the rivers by other means such as bank collapse and creep
508 down slopes. Furthermore, the ^{10}Be concentration of the landslide material is related to grain size
509 with large grains having 3.5 times less ^{10}Be than small grains.

510

511 The difference in isotopic concentration among grain sizes is useful to infer material sourcing.
512 Samples with the greatest diameter result from deep-seated landslides, and carry less ^{10}Be than
513 surface materials. Bedrock landslides can carve deeper than the attenuation length of secondary
514 cosmic rays, bringing to the surface material that has considerably less ^{10}Be content (Niemi et al.,

515 2005). On the other hand, fine-grained material is preferentially sourced from near the land
516 surface, and thus its isotopic concentration is greater.

517

518 This relationship was also found in Puerto Rico by Brown et al. (1998). In a study of chemical
519 and physical erosion in Puerto Rico, Riebe et al. (2003) observed that ^{10}Be concentrations
520 decrease with increasing fractions of coarse material for stream sediments. They attributed this to
521 material sourcing, and suggested that coarse fractions in stream sediments are derived from deep
522 landslides. Given that Puerto Rico and Panama are similar in climate, it is possible that this
523 inverse relationship between ^{10}Be concentration and grain size will be only seen in such steep,
524 wet environments (Bierman et al., unpublished data).

525

526 **5. Conclusions**

527

528 This work presented the first determination of long-term erosion rates in Panama, at the country
529 scale, using cosmogenic nuclides. Erosion rates range from $26.1 \pm 0.6 \text{ m/Myr}$ to 597 ± 62
530 m/Myr . The great variability in erosion and its lack of relationship to topography suggests a
531 complexity in erosive dynamics that is not possible to explain with the metrics we considered.

532

533 Based on their sediment yield calculations, Nichols et al. (2004) estimated that the main reservoir
534 supplying water to the Panama Canal would decrease its capacity by 69% in 600 years. Our data
535 were not compared to theirs, because some of differences in watershed delineation. If this is not

536 addressed correctly, comparisons are invalid. Future work should include correcting this
537 discrepancy in watershed delineation, in order to compare our results to Nichols et al. (2004).
538 This will allow us to explore any changes in reservoir storage capacity based on our erosion
539 rates.

540

541 Panama has erosion rates that are high when compared to other tropical regions where
542 cosmogenic nuclides studies have taken place. The lack of relationships between physiographic
543 variables and erosion rates found in this study suggests that there are other factors at play in
544 controlling erosion at Panama. Seismicity seems to be an important control of erosion, as shown
545 by the relationships found between seismic events and events magnitude at various distances off
546 the watersheds.

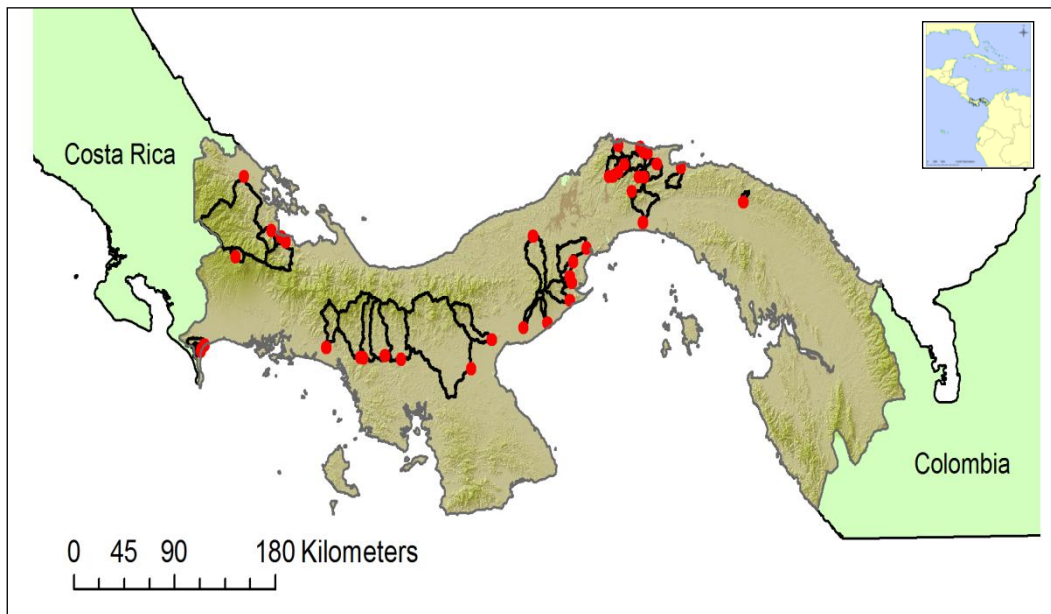


Figure 1: Location of samples and delineated watersheds across Panama. Sampling locations (n=40) are indicated with red dots, and the watersheds draining to them have been delineated and are outlined. Map data from CGIAR-CSI.

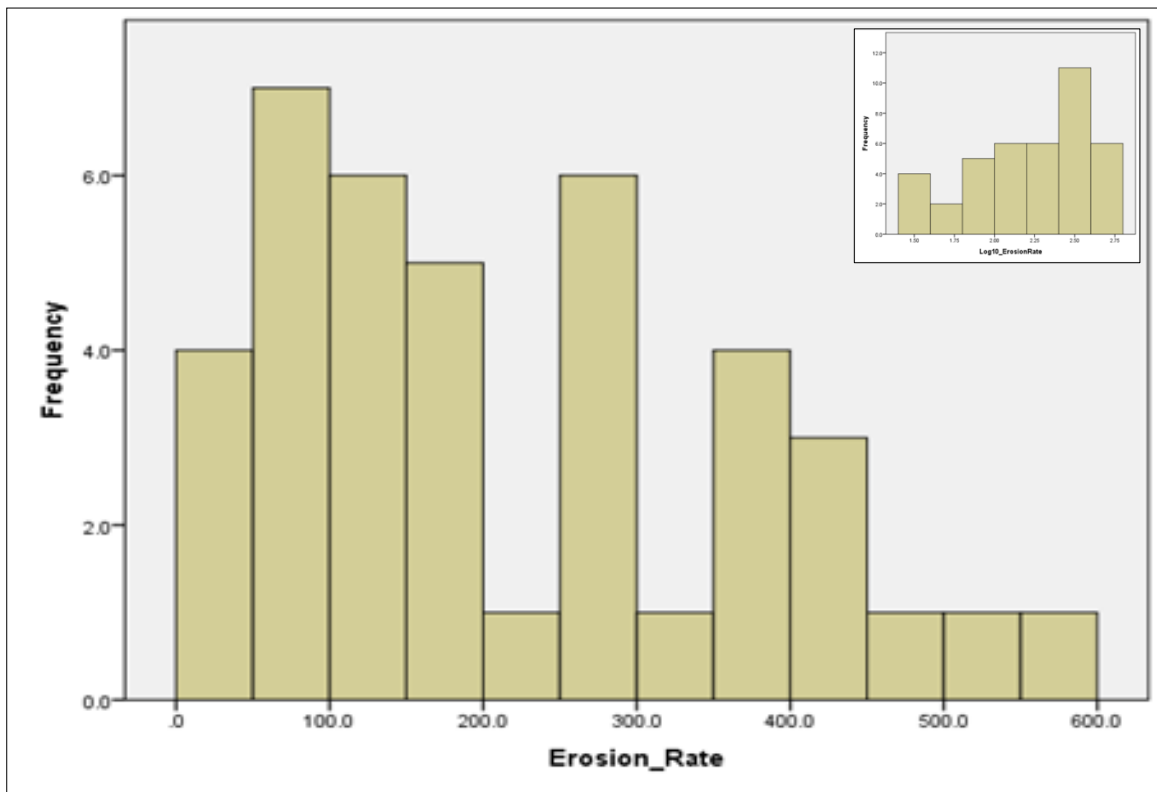


Figure 2: Erosion rate distribution. Erosion rates are highly skewed and do not follow a normal distribution. Skewness in the distribution is reduced after erosion rates are logarithmically (base 10) transformed, and the distribution approaches normality. Transformed erosion rates were used for parametric analysis.

SAMPLE ID	River	Region	Northing	Easting	^{10}Be content ($\times 10^3$ atoms/g)	Erosion rate (m/Myr)
ANT	Anton	Central-East	928349	581595	22.7 ± 0.8	175 ± 7
BART	Bartolo	Southwest	916325	296212	7.4 ± 1.7	505 ± 120
BLA	Boquerón- Outlet	Eastern	1035402	657862	15.1 ± 1.3	258 ± 22
C_NATA	Chico near Nata	Central	919929	553005	137.0 ± 2.6	27.4 ± 0.5
CAIM	Caimito	Central-East	984975	637879	95.4 ± 1.8	34.1 ± 0.7
CAPI	Capira	Central-East	964402	622520	34.8 ± 0.7	115 ± 2
CHAG2009	Chagres Headwaters	Eastern	1034979	689087	68.1 ± 1.7	60.6 ± 1.6
CHAME	Chame	Central-East	947518	622722	23.7 ± 2.0	168.2 ± 14.2
CHAN	Changuinola	Northwest	1035839	331670	39.4 ± 1.2	160 ± 5
CHVIE_H	Chiriquí Viejo Headwaters	Northwest	978626	324237	36.1 ± 1.3	284 ± 10
CNGO	Cuango	Eastern	1056452	685595	14.3 ± 1.2	262 ± 22
COBRE	Cobre	Central	908408	457641	51.7 ± 2.2	75.8 ± 3.4
CORO	Corotu	Southwest	913112	293805	7.9 ± 0.6	459 ± 33
CUAN	Cuango	Eastern	1053293	688405	10.5 ± 0.8	366 ± 29
CUL	Culebra	Eastern	1052186	692279	13.1 ± 1.0	291 ± 23
DIOS	Nombre de Dios	Eastern	1057813	666135	8.3 ± 1.7	441 ± 92
FELIX	Felix	Central	914518	405028	8.0 ± 0.8	597 ± 62
GLOR	La Gloria	Northwest	993157	364491	35.4 ± 1.5	124 ± 5
GRUMO	Guarumo	Northwest	989538	369257	17.6 ± 1.0	283 ± 16
GUAN	Guanabano	Southwest	911892	293354	9.8 ± 1.2	367 ± 46
GUI	Guias	Central-East	931896	602809	18.1 ± 0.6	221 ± 8
IND	Indio	Central-East	993439	590052	66.4 ± 1.8	54.1 ± 1.5
MAND	Mandinga	Eastern	1044547	700401	19.6 ± 0.7	192 ± 7
MARIA	Santa Maria	Central	899354	534672	55.6 ± 1.3	68.0 ± 1.6
NDD	Nombre de Dios	Eastern	1058344	666294	9.0 ± 1.4	403 ± 62
PACORA	Pacora	Eastern	1003367	688077	10.9 ± 0.5	366 ± 18
PAN02	Carti Grande	Eastern	1041964	722329	31.7 ± 0.9	116 ± 3
PAN06	Brazos de Diablo	Eastern	1017356	777490	36.1 ± 0.9	107 ± 3
PERE	Perequete	Central-East	975402	625864	112.4 ± 2.1	29.1 ± .6
PHW	Pequini Headwaters	Eastern	1043899	671363	10.5 ± 1.5	378 ± 56
PLA	Pequini- Outlet	Eastern	1035529	660978	9.4 ± 0.6	417 ± 28
PLS	Upper Chagres	Eastern	684394	1035285	34.6 ± 0.7	121 ± 3
PSM	Pequini	Eastern	1038574	666242	12.4 ± 0.9	319 ± 24
ROBO	Robalo	Northwest	997213	356281	30.5 ± 0.9	148 ± 5
SAJ	Sajlices	Central-East	960284	624479	138.7 ± 3.1	26.1 ± 0.6
SAN_T	San Cristobal	Eastern	1025128	678293	57.6 ± 1.4	76.2 ± 1.9
SANPAB	San Pablo	Central	906069	472211	31.8 ± 0.7	134 ± 3
SMP	San Miguel	Eastern	1038660	666261	14.5 ± 1.7	268 ± 33
TABA	Tabasara	Central	907203	435575	61.9 ± 2.5	78.2 ± 3.2
VIGUI	Vigui	Central	906818	438230	50.1 ± 1.5	88.2 ± 2.6

Table 1: Sample locations are based in NAD 27-Canal Zone. Measured ^{10}Be in the samples is expressed in 1,000 atoms/g. CRONUS Earth Calculator was used to calculate erosion rates. The internal uncertainty calculated by CRONUS is expressed as the uncertainty of each erosion rate. Isotopic data standardized to KNSTD2007 with assumed ratio at 2850×10^{-15}

Region	Average ^{10}Be (x 10^3 atoms/g)	Average erosion rate (m/Myr)	Average basin area (km 2)
Southwestern (n= 3)	8.37 ± 1.27	444 ± 70	34 ± 28
Northwestern (n= 5)	31.8 ± 8.55	200 ± 77	476 ± 752
Central (n= 7)	56.6 ± 39.8	153 ± 199	783 ± 815
Central-east (n= 8)	64.0 ± 46.6	103 ± 77	142 ± 141
Eastern (n= 17)	18.7 ± 15.0	264 ± 151	84 ± 64

Table 2: Regional clustering data. Isotopic content, erosion rates and area for each region were averaged, and the standard deviation was calculated and is expressed as the standard deviation of the measurements.

The number of watersheds in each region is indicated on the first column.

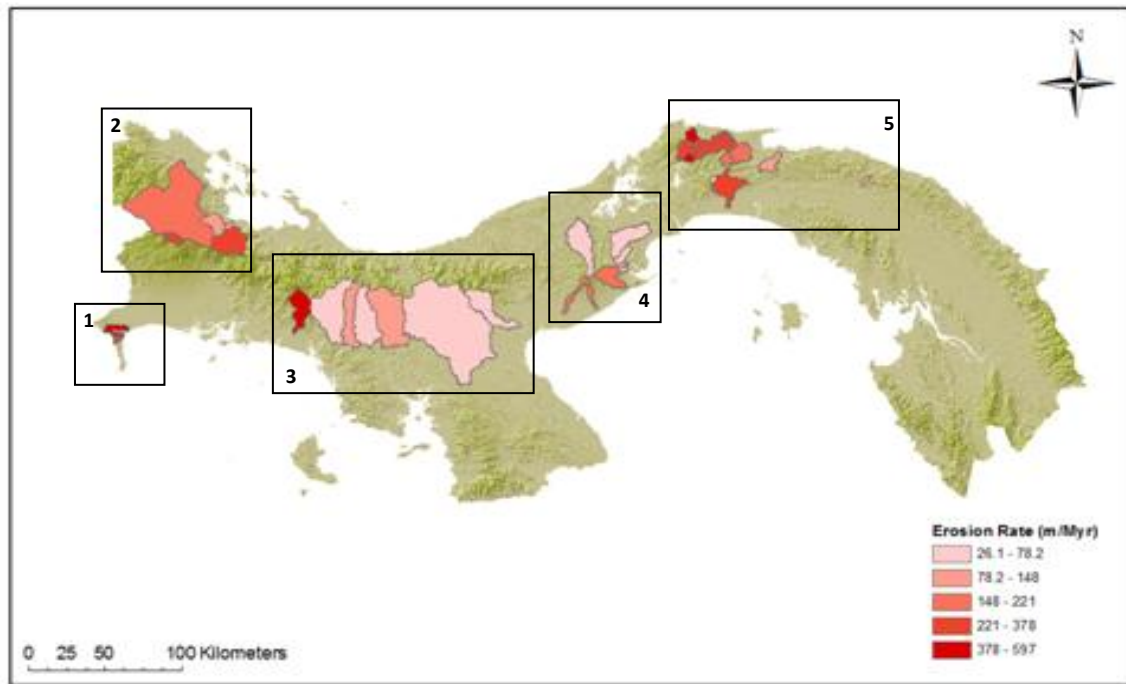


Figure 3: Spatial distribution of erosion rates. There is no spatial pattern of the erosion rates across Panama. Rapidly eroding watersheds are scattered through the country. For regional analysis, samples were divided into 5 groups: Southwestern (box 1), Northwestern (2), Central (3), Central-East (4), and Eastern (5). In order to perform ANOVA at the regional scale, watersheds were classified using the number assigned to each geographical region in this figure.

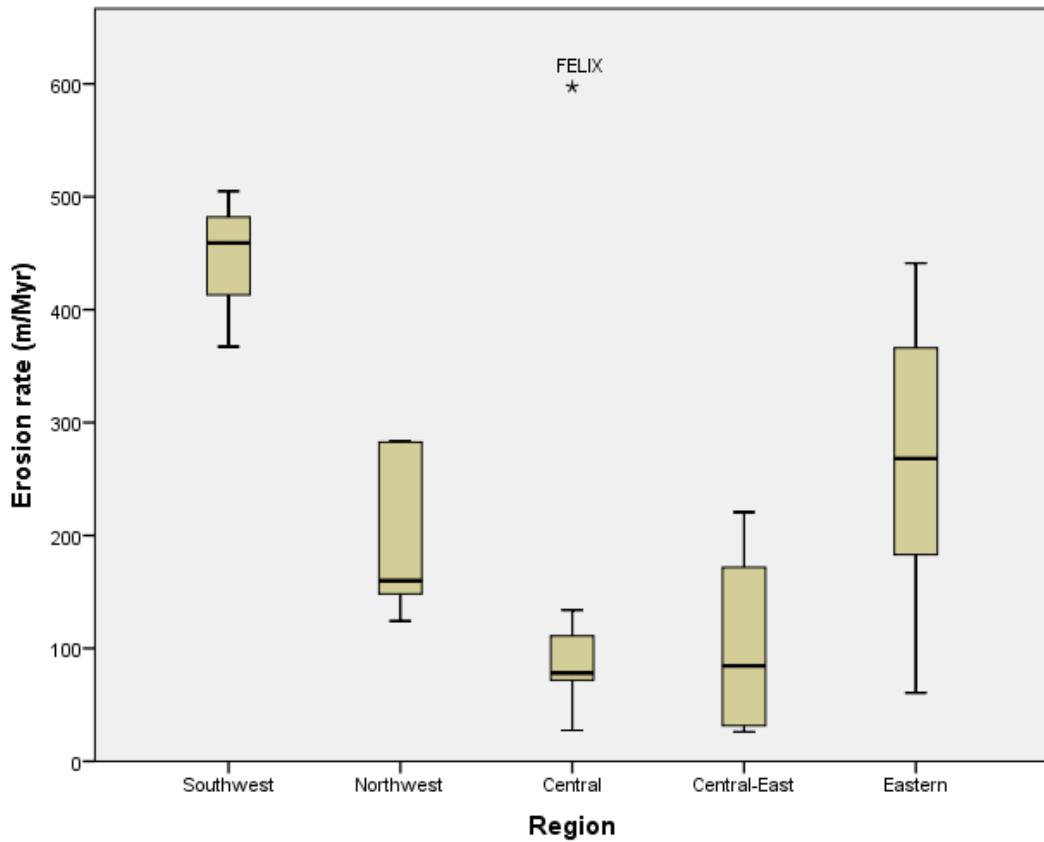


Figure 4: Average erosion by region. The lines inside the boxes represent the median of each region. Horizontal lines in the bars represent the minimum and maximum values for each region. The southwestern region has the highest average erosion rate, and the central region has the highest variability. Rio Felix, represented by an asterisk, is an extreme outlier in our dataset.

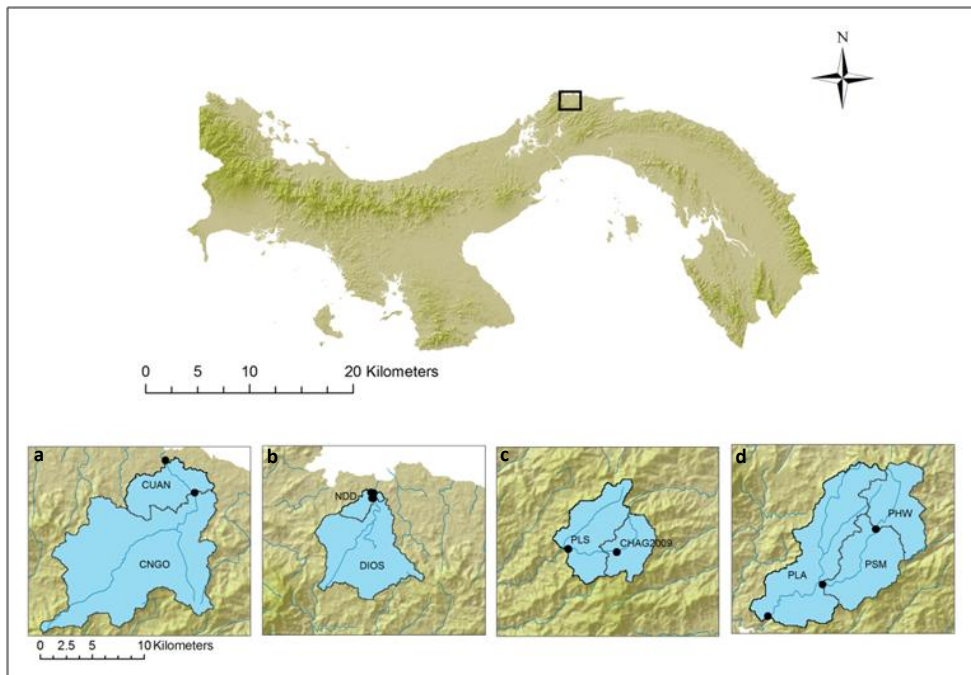


Figure 5: Spatial replicate samples. Nested watersheds for rivers that were sampled more than once along their length: Rio Cuango (a), Rio Nombre de Dios (b), Rio Chagres (c), and Rio Pequini (d). Black dots represent the sample locations. Black box outlines the area where all nested watersheds are located.

River	Sample name	Distance between samples (km)	Sample collection year	^{10}Be concentration ($\times 10^3$ atoms/g)	Erosion Rate (m/Myr)	% SD erosion rates within each river	Subwatershed area (km 2)
Nombre de Dios	NDD	0.55	2004	9.0 ± 1.4	403 ± 62	6	62.46
	DIOS		2007	8.3 ± 1.7	441 ± 92		56.6
Cuango	CNGO		2007	14.3 ± 1.2	262 ± 22		27.49
	CUAN	4.20	2004	10.5 ± 0.8	366 ± 29	23	142.04
Pequini	PHW		2004	10.5 ± 1.5	378 ± 56		34.21
	PLA	13.3 (PHW-PLA)	2004	9.4 ± 0.6	417 ± 28		35.14
	PSM	7.40 (PHW-PSM)	2004	12.4 ± 0.9	319 ± 24	13	76.06
Upper Chagres	CHAG2009	4.7 (CHAG2009-PLS)	2009	68.1 ± 1.7	60.6 ± 14.2		21.27
	PLS		2009	23.2 ± 0.7	183 ± 68	71	56.57

Table 3: Nested watersheds summarized data. Distances were measured in ArcGIS. Percent standard deviation was calculated for each river. Area for each subwatershed was calculated based on a 90-m SRTM DEM using Matlab.

River	Sample Name	Erosion Rate (m/Myr)	Subwatershed Area (km ²)	Erosion between Watersheds (m/Myr)
Nombre de Dios	NDD	403 ± 62	58.60	215
	DIOS	441 ± 92	53.05	
Cuango	CNGO	262 ± 22	158.05	269
	CUAN	366 ± 29	132.18	
Upper Chagres	CHAG2009	60.6 ± 14.2	20.11	250
	PLS	183 ± 68	56.57	
Pequini (A)	PHW	378 ± 56	32.06	270
	PSM	319 ± 24	70.76	
Pequini (B)	PSM	319 ± 24	70.76	509
	PLA	417 ± 28	146.18	
Pequini (C)	PHW	378 ± 56	32.06	428
	PLA	417 ± 28	146.18	

Table 4: Erosion rates for the area between subwatersheds were calculated using the equation presented by Granger et al. (1996): $E_{2-1} = E_2 A_2 - E_1 A_1 / A_2 - A_1$, where A is the Area and E the erosion rate of the subcatchments, obtained from Matlab and CRONUS, respectively. These data was used to calculate the erosion rate of the area between two samples. A_1 and E_1 represent the area and erosion of the watershed delineated from the upstream sampling point. Similarly A_2 and E_2 represent the sample taken downstream, with reference to A_1 and E_2 .

Variable	R ² (n=40)	R ² (n=5)
Slope	0.009 (p=0.955)	0.192 (p=0.460)
Area	0.223 (p= 0.166)	0.267 (p=0.372)
Relief	0.196 (p= 0.226)	0.353 (p=0.290)
Elevation	0.040 (p= 0.805)	0.186 (p=0.468)
Average Temperature	0.041 (p= 0.800)	0.071 (p=0.666)
Isothermality	0.381 (p= 0.015)	0.164 (p=0.499)
Temperature Seasonality	0.445 (p= 0.004)	0.419 (p=0.237)
Max Temp Warm Month	0.066 (p= 0.686)	0.160 (p=0.504)
Min Temp Cold Month	0.005 (p= 0.676)	0.004 (p=0.921)
Temperature Range	0.019 (p= 0.907)	0.270 (p=0.369)
Temperature Wet Quart	0.074 (p= 0.648)	0.074 (p=0.658)
Temperature Dry Quart	0.037 (p= 0.823)	0.060 (p=0.692)
Temperature Warm Quart	0.026 (p= 0.876)	0.076 (p=0.654)
Temperature Cold Quart	0.084 (p= 0.605)	0.046 (p=0.728)
Annual Precipitation	0.307 (p= 0.054)	0.000 (p=0.973)
Mean Diurnal Range	0.055 (p= 0.737)	0.156 (p=0.511)
Precipitation Wet Month	0.048 (p= 0.771)	0.450 (p=0.215)
Precipitation Dry Month	0.319 (p= 0.045)	0.000 (p=0.981)
Precipitation Seasonality	0.394 (p= 0.012)	0.003 (p=0.936)
Precipitation Wet Quart	0.045 (p= 0.784)	0.083 (p=0.638)
Precipitation Dry Quart	0.376 (p= 0.017)	0.003 (p=0.928)
Precipitation Warm Quart	0.292 (p= 0.068)	0.005 (p=0.913)
Precipitation Cold Quart	0.023 (p= 0.889)	0.027 (p=0.792)
Tree Cover	0.351 (p= 0.026)	0.417 (p=0.239)
Chemical Weathering	0.726 (p= 0.004)	-
Peak Ground Acceleration	0.307 (p= 0.054)	0.589 (p=0.130)
Surface Geology	F = 2.427 (p= 0.102)	-
Seismic Events 100m	0.184 (p= 0.256)	0.392 (p=0.258)
Average Depth 100m	0.128 (p= 0.430)	0.028 (p=0.786)
Average Magnitude 100m	0.155 (p= 0.340)	0.074 (p=0.658)
Seismic Events 10km	0.338 (p= 0.033)	0.813 (p=0.036)
Average Depth 10km	0.140 (p= 0.389)	0.302 (p=0.338)
Average Magnitude 10km	0.220 (p= 0.172)	0.196 (p=0.456)
Seismic Events 25km	0.350 (p= 0.027)	0.474 (p=0.199)
Average Depth 25km	0.334 (p= 0.035)	0.477 (p=0.196)
Average Magnitude 25km	0.431 (p= 0.005)	0.679 (p=0.086)
Seismic Events 50km	0.363 (p= 0.021)	0.706 (p=0.075)
Average Depth 50km	0.466 (p= 0.002)	0.450 (p=0.215)
Average Magnitude 50km	0.368 (p= 0.019)	0.173 (p=0.486)
Seismic Events 75km	0.348 (p= 0.028)	0.389 (p=0.157)
Average Depth 75km	0.420 (p= 0.007)	0.390 (p=0.260)
Average Magnitude 75km	0.550 (p= 0.000)	0.407 (p=0.247)
Average Depth 100km	0.198 (p= 0.221)	0.286 (p=0.354)
Average Magnitude 100km	0.352 (p= 0.026)	0.407 (p=0.247)
Seismic Events 100km	0.316 (p= 0.047)	0.179 (p=0.478)

Table 5: Regression coefficients for erosion and analyzed variables. Column two presents the results for the global analysis, including all watersheds individually. Results for regional analysis, when samples were grouped and the sample number is reduced to five, are presented in column three. All parametric analyses were performed with \log_{10} transformed erosion data. Fields in italics represent relationships that are not statistically significant at the 0.05 significance level. For regional analysis, the number of seismic

events is the sum of the events in all watersheds. For all other parameters, values were averaged. No analysis was done for surface geology at the regional scale, because only two categories were present when samples were grouped. Sedimentary rocks are not represented. No chemical weathering analysis was done at the regional scale. The 9 watersheds that have silicate weathering data are not representative of all regions.

Variable	R ²	p	Slope of line
Events 100m	0.184	0.256	0.006
Depth 100m	0.128	0.760	-0.002
Magnitude 100m	0.155	0.340	-0.026
Events 10km	0.338	0.033	0.001
Depth 10km	0.140	0.389	-0.001
Magnitude 10km	0.220	0.172	0.050
Events 25km	0.350	0.027	0.001
Depth 25km	0.334	0.035	-0.005
Magnitude 25km	0.431	0.005	-0.165
Events 50km	0.363	0.021	0.000
Depth 50km	0.466	0.002	-0.008
Magnitude 50km	0.368	0.019	-0.361
Events 75km	0.348	0.028	0.0000
Depth 75km	0.420	0.007	-0.012
Magnitude 75km	0.550	0.000	-1.359
Events 100km	0.316	0.047	0.000
Depth 100km	0.198	0.221	-0.006
Magnitude 100km	0.352	0.026	-1.080

Table 6: Seismic variables and their relation to erosion. Regional analyses of the relationship between seismic variables and erosion is included in table 5. Seismicity variables (number of events, average depth and average magnitude) were quantified in the six arbitrarily selected buffers shown in column one. The strength of the relationship between any given variable and erosion is presented in column two and p-value in column three. The slope of the line is presented in the last column four. Fields in italics represent relationships that are not statistically significant at the 0.05 significance level.

River (sample ID)	Silicate weathering ¹ (t km ⁻² yr ⁻¹)	Sediment yield (t km ⁻² yr ⁻¹)	Percent of Silicate in sediment yield
Anton (ANT)	38.6	474	8.2
Chagres (CHAG2009)	20.8	164	12.7
Chiriqui Viejo (CHVIEH)	42.7	766	5.6
Chico (C-NATA)	13.8	73.9	18.7
Cobre (COBRE)	26.2	205	12.8
Felix (FELIX)	34.2	1613	2.1
San Pablo (SANPAB)	26.9	362	7.4
Tabasara (TABA)	23.7	211	11.2
Vigui (VIGUI)	26.5	239	11.1

Table 7: Comparison of sediment yield and silicate weathering rates in Panama. Silicate weathering was measured by Steven Goldsmith and Russell Harmon (unpublished data)

Isotopic concentration relation to grain size

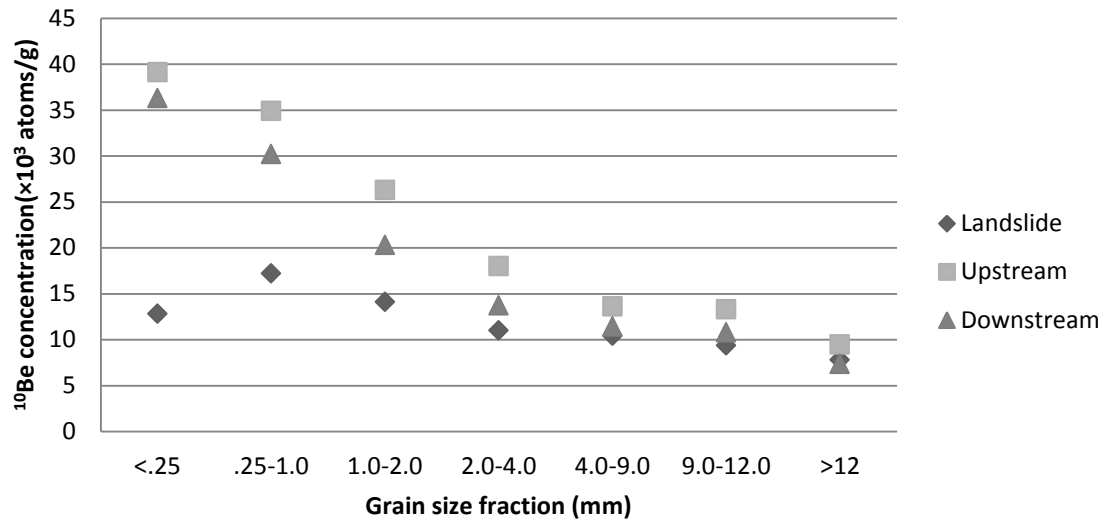


Figure 6: Isotopic concentration variation with grain size. Two general trends can be identified from the grain size fractions of our data. First, ¹⁰Be concentration decreases as grain size increases, except for the coarser size fraction (>12mm). Also, material from the landslide (PLSS) almost always has the lowest isotopic concentration of each grain size fraction.

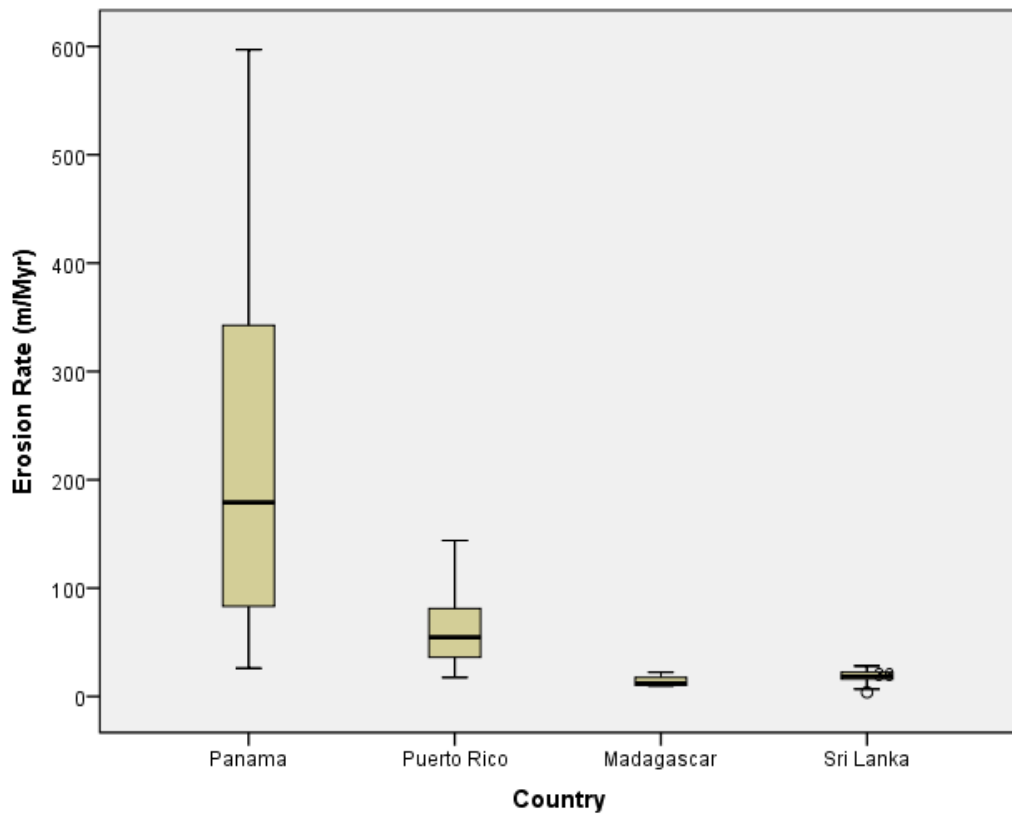


Figure 7: Comparison of cosmogenic-determined erosion rates in tropical climates. Bottom and top of the boxes represent the lower and upper quartile, respectively. Lines inside the boxes represent the median erosion rate of published data for each country. The minimum and maximum erosion rates are represented by the horizontal lines in the bars. In Panama, erosion rates averaged 218 m/Myr (n=40), in Puerto Rico averaged 60.9 m/Myr (n=24). Erosion rate averaged 18.1 m/Myr in the 4 watersheds studied in Madagascar, and 13.9 m/Myr in Sri Lanka (n=16). Panama data previously published by Nichols et al. (2005) is not included in this figure.

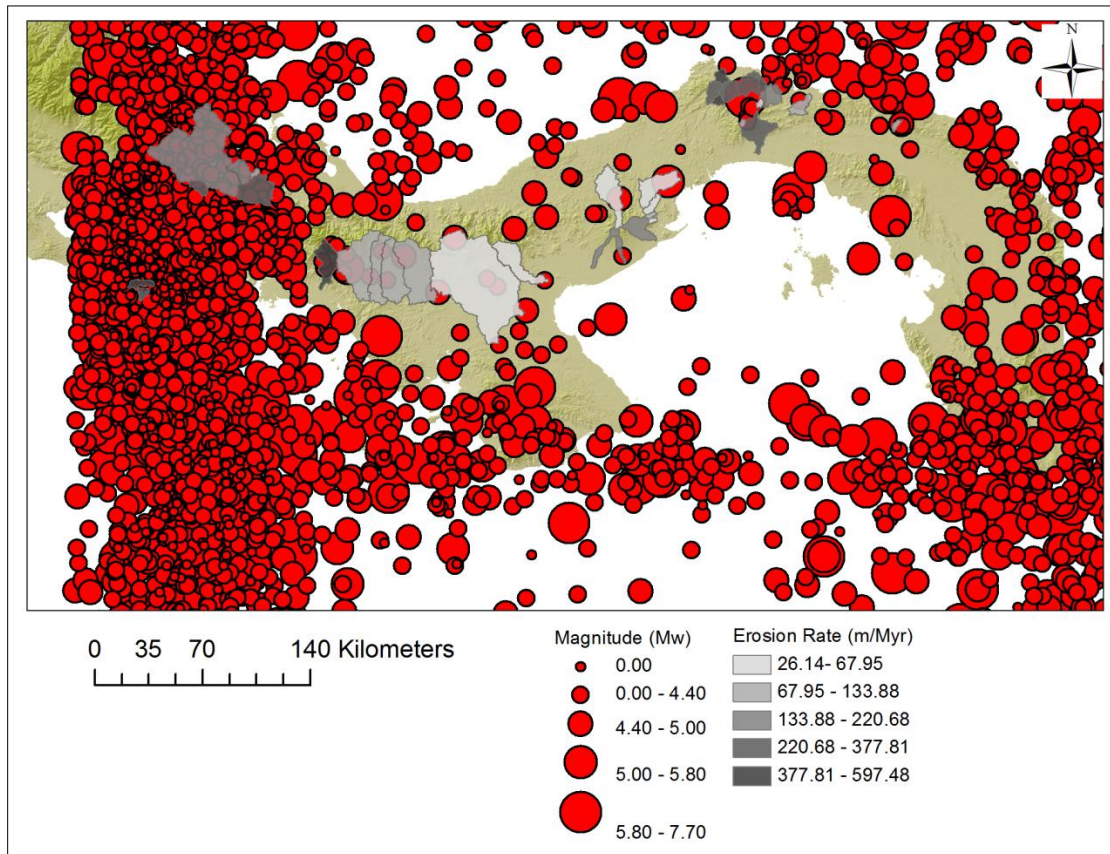


Figure 8: Seismic activity in Panama. Circles represent individual seismic events (1900-2011). Circle size is representative of the event magnitude. Watershed color is representative of erosion rate. Location of Rio Felix, with the highest erosion rate in our dataset, is marked with the black box. Seismic data provided by the Instituto de Geociencias (Eduardo Camacho, personal communication).

Paper references→NEED JOURNAL FORMATTING!(Also, check order specially for multiple works from same author)

Adamek, S., C. Frolich, and W. Pennington. "Seismicity of the Caribbean-Nazca Boundary: Constraints on Microplate Tectonics of the Panama Region." *Journal of Geophysical Research* 93 (1988): 2053-75.

Bierman, P.R., and Kyle Keedy Nichols. "Rock to Sediment—Slope to Sea With ^{10}Be —Rates of Landscape Change." *Annual Review of Earth and Planetary Sciences* 32, no. 1 (2004): 215-55.

Bilotta, G. S., and R. E. Brazier. "Understanding the Influence of Suspended Solids on Water Quality and Aquatic Biota." [In eng]. *Water Res* 42, no. 12 (Jun 2008): 2849-61.

Brown, Erik T., Robert F. Stallard, Matthew C. Larsen, Didier Bourles, L., Grant M. Raisbeck, and Francoise Yiou. "Determinarion of Predevelopment Denudation Rates of an Agricultural Watershed (Cayaguás River, Puerto Rico) Using in-Situ Produced ^{10}Be in River-Borne Quartz." *Earth and Planetary Science Letters* 160 (1998): 723-28.

Brown, Erik T., Robert F. Stallard, Matthew C. Larsen, Grant M. Raisbeck, and Francoise Yiou. "Denudation Rates Determined from the Accumulation of in-Situ Produced ^{10}Be in the Luquillo Experimental Forest, Puerto Rico." *Earth and Planetary Science Letters* 129 (1995): 193-202.

Camacho, E., C. Lindholm, A. Dahle, and H. Bungum. "Seismic Hazard Assessment in Panama." *Engineering Geology* 48 (1997): 1-6.

Cox, Rónadh, Paul Bierman, Matthew C Jungers, and A. F Michel Rakotondrazafy. "Erosion Rates and Sediment Sources in Madagascar Inferred From ^{10}Be Analysis of Lavaka, Slope, and River Sediment." *The Journal of Geology* 117, no. 4 (2009): 363-76.

Davidson, D. "Recent Uplift of the Burica Peninsula, Panama and Costa Rica, Recorded by Marine Terraces." Honors Thesis, Trinity University 2010.

Gosse, John C., and Fred M. Phillips. "Terrestrial in Situ Cosmogenic Nuclides: Theory and Application." *Quaternary Science Reviews* 20 (2001): 1475-560.

Harden, Carol P. "Human Impacts on Headwater Fluvial Systems in the Northern and Central Andes." *Geomorphology* 79, no. 3-4 (2006): 249-63.

Harmon, R. S. "Geological Development of Panama." In *The Río Chagres, Panama: A Multidisciplinary Profile of a Tropical Watershed*, edited by R. S. Harmon. 354. Netherlands: Springer, 2005.

Hewawasam, Tilak, Friedhelm von Blanckenburg, M. Schaller, and Peter Kubik. "Increase of Human over Natural Erosion Rates in Tropical Highlands Constrained by Cosmogenic Nuclides." *Geology* 31, no. 7 (2003): 597-600.

Hunt, A. L., G. A. Petrucci, P. R. Bierman, and R. C. Finkel. "Metal Matrices to Optimize Ion Beam Currents for Accelerator Mass Spectrometry." *Nuclear Instruments and Methods in Physics Research Section B: Beam Interactions with Materials and Atoms* 243, no. 1 (2006): 216-22.

Kohl, C. P., and K. Nishiizumi. "Chemical Isolation of Quartz for Measurement of in-Situ Produced Cosmogenic Nuclides." *Geochimica et Cosmochimica Acta* 56 (1992): 3583-87.

Lal, D., and B Peters. "Cosmic-Ray Produced Radioactivity on the Earth." In *Handbuch Der Physik*, edited by K. Sitte. 551-612. New York: Springer-Verlag, 1967.

Malusà, Marco G., and Giovanni Vezzoli. "Interplay between Erosion and Tectonics in the Western Alps." *Terra Nova* 18, no. 2 (2006): 104-08.

Milliman, J. D., and J. P. Syvitski. "Geomorphic/Tectonic Control of Sediment Discharge to the Ocean: The Importance of Small Mountainous Rivers." *The Journal of Geology* 100 (1992): 525-44.

Nichols, Kyle K., Paul R. Bierman, Robert Finkel, and Jennifer Larsen. "Long-Term (10 to 20 Kyr) Sediment Generation Rates for the Upper Rio Chagres Basin Based on Cosmogenic ^{10}Be ." In *The Rio Chagres, Panama: A Multidisciplinary Profile of a Tropical Watershed*, edited by Russell S. Harmon. 354. The Netherlands: Springer, 2004.

Niemi, Nathan A., Michael Osokin, Douglas W. Burbank, Arjun M. Heimsath, and Emmanuel J. Gabet. "Effects of Bedrock Landslides on Cosmogenically Determined Erosion Rates." *Earth and Planetary Science Letters* 237, no. 3-4 (2005): 480-98.

Ouimet, William B. "Landslides Associated with the May 12, 2008 Wenchuan Earthquake: Implications for the Erosion and Tectonic Evolution of the Longmen Shan." *Tectonophysics* 491, no. 1-4 (2010): 244-52.

Palka, E. J. "A Geographic Overview of Panama." In *The Rio Chagres, Panama. A Multidisciplinary Profile to a Tropical Watershed*, edited by Russell S. Harmon. 3-18. Netherlands: Springer, 2005.

Palumbo, L., R. Hetzel, M. Tao, and X. Li. "Topographic and Lithologic Control on Catchment-Wide Denudation Rates Derived from Cosmogenic ^{10}Be in Two Mountain Ranges at the Margin of NE Tibet." *Geomorphology* 117, no. 1-2 (2010): 130-42.

Panamá, Contraloría General de la República de. "Estadísticas Ambientales: Años 2000-04." edited by Instituto Nacional de Estadística y Censo. Panamá, República de Panamá: Contraloría General de la República de Panamá, 2005.

Panamá, Contraloría General de la República de. "Panamá en cifras: Años 2000-04." edited by Instituto Nacional de Estadística y Censo. Panamá, República de Panamá: Contraloría General de la República de Panamá, 2005.

Panamá, Contraloría General de la República de. "Estadísticas Ambientales: Años 2000-2004." Instituto Nacional de Estadística y Censo, 2008.

Panamá, Contraloría General de la República de. "Plan Nacional de Desarrollo Forestal: Modelo Forestal Sostenible." edited by Autoridad Nacional del Ambiente- ANAM, 2008

Portenga, Eric W., and Paul R. Bierman. "Understanding Earth's Eroding Surface with ^{10}Be ." *GSA Today* 21, no. 8 (2011): 4-10.

Riebe, Clifford S., James W. Kirchner, and Darryl E. Granger. "Quantifying Quartz Enrichment and Its Consequences for Cosmogenic Measurements of Erosion Rates from Alluvial Sediment and Regolith." *Geomorphology* 40 (2001): 15-19.

Riebe, Clifford S., James W. Kirchner, Darryl E. Granger, and R. C. Finkel. "Minimal Climatic Control on Erosion Rates in the Sierra Nevada, California." *Geology* 29, no. 5 (2001): 447-50.

Riebe, Clifford S., James W. Kirchner, and Robert C. Finkel. "Long-Term Rates of Chemical Weathering and Physical Erosion from Cosmogenic Nuclides and Geochemical Mass Balance." *Geochimica et Cosmochimica Acta* 67, no. 22 (2003): 4411-27.

Riebe, Clifford S., James W. Kirchner, and Robert C. Finkel. "Erosional and Climatic Effects on Long-Term Chemical Weathering Rates in Granitic Landscapes Spanning Diverse Climate Regimes." *Earth and Planetary Science Letters* 224, no. 3-4 (2004): 547-62.

Schuchert, C. "Panama." Chap. 37 In *Historical Geology of the Antillean-Caribbean Region or the Lands Bordering the Gulf of Mexico and the Caribbean Sea*. 810. New York: John Wiley & Sons, 1995

von Blanckenburg, Friedhelm. "The Control Mechanisms of Erosion and Weathering at Basin Scale from Cosmogenic Nuclides in River Sediment." *Earth and Planetary Science Letters* 237 (2005): 462-79.

Summerfield, M. A., and N. J. Hulton. "Natural Controls of Fluvial Denudation Rates in Major World Drainage Basins." *Journal of Geophysical Research* 99, no. B7 (1994): 13871-83.

Terry, R. A. *A Geological Reconnaissance of Panama*. San Francisco, CA: California Academy of Sciences, 1956.

Trimble, S.W.. "The Fallacy of Stream Equilibrium in Contemporary Denudation Studies." *American Journal of Science* 277 (1977): 876-87.

Varela, Sara, Jesús Rodríguez, and Jorge M. Lobo. "Is Current Climatic Equilibrium a Guarantee for the Transferability of Distribution Model Predictions? A Case Study of the Spotted Hyena." *Journal of Biogeography* 36, no. 9 (2009): 1645-55.

von Blanckenburg, F., T. Hewawasam, and P.W. Kubik. "Cosmogenic Nuclide Evidence for Low Weathering and Denudation in the Wet, Tropical Highlands of Sri Lanka." *Journal of Geophysical Research* 109, no. F3 (2004).

von Blanckenburg, Friedhelm. "The Control Mechanisms of Erosion and Weathering at Basin Scale from Cosmogenic Nuclides in River Sediment." *Earth and Planetary Science Letters* 237 (2005): 462-79.

West, A., A. Galy, and M. Bickle. "Tectonic and Climatic Controls on Silicate Weathering." *Earth and Planetary Science Letters* 235, no. 1-2 (2005): 211-28.